

MRI Image Overlay: Application to Arthrography Needle Insertion

Gregory S. Fischer¹, Anton Deguet¹, Csaba Csoma¹, Russell H. Taylor¹,
Laura Fayad², John A. Carrino³, S. James Zinreich² and Gabor Fichtinger^{1,2}

¹ Johns Hopkins University, Engineering Research Center, Baltimore, MD, USA

² Johns Hopkins Hospital, Dept. of Radiology, Baltimore, MD, USA

³ Brigham and Women's Hospital, Dept. of Radiology, Boston, MA, USA

ABSTRACT

Magnetic Resonance Imaging (MRI) provides great potential for planning, guiding, monitoring and controlling interventions. MR arthrography (MRAr) is the imaging gold standard to assess small ligament and fibrocartilage injury in joints. In contemporary practice, MRAr consists of two consecutive sessions: 1) an interventional session where a needle is driven to the joint space and MR contrast is injected under fluoroscopy or CT guidance, and 2) A diagnostic MRI imaging session to visualize the distribution of contrast inside the joint space and evaluate the condition of the joint. Our approach to MRAr is to eliminate the separate radiologically guided needle insertion and contrast injection procedure by performing those tasks on conventional high-field closed MRI scanners. We propose a 2D augmented reality image overlay device to guide needle insertion procedures. This approach makes diagnostic high-field magnets available for interventions without a complex and expensive engineering entourage. In preclinical trials, needle insertions have been performed in the joints of porcine and human cadavers using MR image overlay guidance; insertions successfully reached the joint space on the first attempt in all cases.

Keywords: MRI, image overlay, augmented reality, joint arthrography

1 INTRODUCTION AND BACKGROUND

1.1 Interventional MRI

Magnetic resonance imaging is an excellent imaging modality for the detection and characterization of many human diseases. Its outstanding soft tissue contrast allows for accurate delineation of the pathologic and surrounding normal structures. Thus MRI has an unmatched potential for guiding, monitoring and controlling therapy [20, 21]. In needle biopsies, the high sensitivity of MRI in detecting lesions allows excellent visualization of the pathology, and the high tissue contrast helps to avoid critical structures in the puncture route [20, 25]. Advances in magnet design and magnetic resonance (MR) system technology coupled with the development of fast pulse sequences have contributed to the increasing interest in interventional MRI.

There are a number of technical aspects and concerns to consider when putting an interventional magnet into operation. Among the most pertinent ones are: configuration and field strength of the magnet (which necessitates a compromise between access to the patient and signal-to-noise), safety and compatibility of the devices and instruments that will be used in or near the magnetic field, spatial accuracy of imaging for localization and targeting, optimal use of the imaging hardware and software (the dynamic range of gradients, limitation and availability of pulse sequences, radiofrequency coils) and level of integration with guidance methods for accomplishing the procedure.

There are three main magnet bore configurations that are currently used for interventional MR. The first type, "clam shell" configuration, has a horizontally opened gap and is basically an adaptation and slight modification to the routine open low field MR unit.

The second type, "cylinder" configuration, is an adaptation of a high field (1.5T or 3.0T) MR unit. Some are made with a flared opening or wider bore to allow an operator to reach in but, in general does not allow for direct patient access for a majority of procedures without robotic or other mechanical assistance. Therefore imaging and intervention are "uncoupled". That is, manipulation of devices or surgical work is done outside the bore and then the patient must be moved into the magnet for imaging. The third type of configuration is a mid-field (0.5 Tesla) magnet specifically designed for intervention, which has 2 cylinders separated by a gap for access, referred to as the "double donut" (SIGNA SP GE Medical Systems, Milwaukee) but is no longer offered as a commercial product. A wide variety of procedures may be performed on open magnets but the trend is to use high field closed magnets [32], mainly because of improved imaging quality and wider availability of pulse sequences. The higher the field the higher the signal to noise ratio (SNR), and the higher SNR can be used to improve spatial and temporal resolution and can make techniques like temperature or flow sensitive imaging, functional brain MRI, diffusion imaging or MR spectroscopy more useful. Considering these trends, it appears that the use of conventional high-field closed MRI scanners for guidance will allow more successful dissemination of MR-guided techniques to radiology facilities throughout the country and eventually beyond.

We propose 2D image overlay to guide the needle insertion in procedures where real-time imaging update is not strictly necessary, so one can translate the patient out of the gantry between imaging and needle insertion. This approach can make diagnostic high-field magnets available for interventions without involving prohibitively complex and expensive engineering additions. Clinical applications highly suitable for this technique include musculoskeletal procedures such as arthrography, as well as biopsy and spine injections. MR-guided interventional procedures involving bone, soft tissue, intervertebral discs, and joints are feasible, safe and efficacious. In these applications, clinical success is directly linked to spatial accuracy. Faulty needle placement may also injure sensitive structures, thus exposing the patient to risk and pain. However, the ultimate effectiveness and adoption of these techniques will depend upon the availability of a simple and robust system, similar in complexity to CT and US guided interventions.

Limitations of conventional free-hand needle placement include the operator's ability to maintain the correct trajectory toward the target, thus causing increased number of needle passes (iterations). Typically, the guidance images are displayed on the operator's 2D console, on which the operator plans the intervention. Then the operator mentally registers the images with the anatomy of the patient, and uses hand-eye coordination to execute the planned intervention. Practitioners generally agree that, given enough time and opportunity for intermittent imaging and adjustments, the target usually can be reached with appropriate accuracy. The important question is, however, whether the same objective could be achieved with fewer insertion attempts, because each needle correction requires acquisition of extra images and reinsertion of the needle, thereby increasing the risk of complication, discomfort, and the length of the pro-

cedure. Hence the prime objective of our research is maximizing accuracy while minimizing faulty needle insertion attempts under MR guidance.

1.2 MRI-Guided Joint Arthrography

Adequately depicting internal derangements of joints have been a challenge for medical imaging. Currently this evaluation has been improved by the use of MR arthrography (MRAr) [36]. MRAr may be accomplished by way of a percutaneously placed needle approach (referred to as direct MRAr) or with an intravenous injection of a gadolinium based material (referred to as indirect MRAr). For any joint, the placement of intra-articular contrast (by direct or indirect means) can be utilized to assist the evaluation of ligaments, cartilage, synovial proliferation or loose intra-articular bodies. MRAr is most commonly used in the shoulder, hip and knee. However, there are also good indications for elbow, wrist and ankle MRAr.

Direct MRAr has become a well-established method of delineating various joint structures that otherwise show poor contrast with conventional MRI. Direct MRAr is well tolerated and has comparable diagnostic efficacy to joint arthroscopy, the gold standard in the evaluation of joints [35, 34]. The main advantages of direct MRAr are the reliable and consistent arthrographic effect and capsular distension produced. However, direct MRAr necessitates image guidance for joint injection, traditionally with fluoroscopy or sometimes under CT guidance [2]. Thus current direct MRAr comprises two distinct procedures: an initial radiologically-guided needle injection intervention that is promptly followed by a second diagnostic MRI session before the contrast becomes resorbed. Such a tightly sequenced double-procedure makes contemporary direct MRAr more expensive, resource intensive, and difficult to schedule. To address this problem, [18] and [30] reported the use of open MRI scanner configuration where needle insertion and contrast injection were performed directly inside scanner in the same setting. Lewin et al. in [31], and later [23] and [11] reported the use of "open C-arm scanner" which consists of a vertically open MRI and optically co-registered C-arm fluoroscope. This approach also eliminated the double scheduling problem by bringing fluoroscopically guided contrast injection and MR-guided joint evaluation into the same room, but at the expense of a complex and expensive engineering entourage, which is neither practical nor generalizable.

Indirect MRAr has developed as an alternative to direct MR arthrography for imaging joints in part to obviate the intra-articular needle injection. The main advantage supporting the use of indirect MRAr is no necessity for a fluoroscopy suite. Indirect MRAr, however, can require a longer patient visit because of the time delay between injection and imaging needed to provide suitable intra-articular enhancement. Interpretative error may result from the enhancement of extra-articular structures (such as vessels, tendon sheaths, and bursae), which may be confounded for extravasated contrast material from the joint [41, 1]. Another limitation of indirect MR arthrography is a lack of controlled joint distension compared with that of direct arthrography [41, 1]. Joint distension facilitates recognition of certain conditions such as capsular trauma or soft tissue injury concealed by a collapsed capsule. Indirect MRAr is often performed when direct arthrography is inconvenient or not logistically feasible.

Thus far only limited work has been done using MR imaging as guidance for the needle and contrast placement for MRAr. A cadaver based study showed an MR-guided technique in conjunction with the LCD screen and real-time MR imaging would be a practical alternative to conventional fluoroscopic guidance [39]. A case series involving human subjects showed the feasibility of MR-guided MRAr in the shoulder using an open configuration magnet with rapid or real-time imaging [18]. However, with low field magnets that have a vertically oriented main magnetic field, the tradi-

tional radiologic approach to the shoulder must be modified to provide adequate visualization of the needle [31]. MR-guided shoulder MRAr has also been performed on conventional high field closed bore magnet requiring several passes for joint cavity puncture [40]. An extension of this paradigm is to use a robust facile economical targeting system to facilitate joint cavity puncture.

Our approach to direct MRAr is to eliminate the separate radiologically guided needle insertion and contrast injection task from the procedure by performing those tasks directly on conventional high-field closed MRI scanner using the MR image overlay technique. The hypothesis is that the image overlay technique allows for accurate, safe, and fast needle placement and contrast injection. This promises to reduce the inconvenience for the patient and logistical difficulties associated with current direct MRAr, in a manner that is practical and affordable for any facilities that own conventional MRI scanners.

1.3 Surgical Assistant Techniques

A variety of MR-compatible surgical robots including [9, 24, 17, 5, 6, 28] have been investigated to assist image guided insertions; all resulting in systems that are custom-made for one particular application and/or prohibitively complex and expensive for routine clinical use. Numerous surgical navigation systems (SNS) have been developed to aid the operator by tracking the surgical tool with respect to the imaging device by dynamically referencing some fiducials (skin markers, bone screws, head-frame, etc.) attached to the patient's body. Although SNS have been commercially available for over a decade, they were not applied in the scanner room except in a handful of limited trials with low-field open MRI [26, 27, 31, 11, 23]. While the application of SNS on high-field closed MRI might seem obvious from certain perspectives, such a transition has not yet been witnessed. The explanation of this can be found in the inherent limitations of tracked SNS. In theory, the most appealing aspect of tracked SNS is multiplanar image guidance, i.e. when the needle trajectory is shown in three orthogonal images reformatted in real-time as the needle moves: the tool is unconstrained while real-time images follow the tool. This feature is excellent, as long as the reformatted images are of good quality, i.e. the image volume is large along all three dimensions and the voxel resolution is uniformly high. SNS also works well on open magnets [26, 27] where the acquisition of MR slices follow the tool in real-time. This, however, is not the case with closed bore magnets where patients are moved in and out of the bore for needle manipulation. In these procedures, in the interest of time, we acquire only a few thin slices (often only a single image) instead of a thick and dense slab of data. This limitation has a decisive negative impact on the performance of SNS, because real-time image reformation is now impossible outside the principal plane of imaging (which is typically the transverse plane), thereby depriving the SNS of its best feature. Therefore, the surgical tool (needle) is constrained to a thin image slab or single image. Further problems include that optical trackers require unobstructed line of sight that may result in a spatial arrangement disrupting room traffic; and that electromagnetic trackers are incompatible with the MRI room altogether. In short, tracked SNS are not well suited for assisting interventions on closed bore high-field MRI scanners.

In an attempt to fuse imaging information with the operative field, several augmented reality and optical guidance techniques have been investigated. Birkfellner et al. integrated computer graphics into the optical path of a head-mounted stereo binocular [3]. Sauer et al. reported another variant of head-mounted display (HMD) technology [33], in which two head-mounted cameras captured the real scene and a stereo HMD visualized the augmented scene. Edwards et al. describe image overlay for microscope-assisted guided interventions [10]. DiGioia et al. developed a volumetric image overlay system by projecting 3-D virtual image on a

semitransparent mirror in which the physician simultaneously can observe the actual patient and computer-generated images [4, 8]. A similar device using this concept is commercially available under the brand name of Dexteroscope [22], which also involves elaborate preoperative calibration and requires real-time spatial tracking of all components, including the patient, physicians head, overlay display, mirror, and surgical tools. Grimson et al. graphically overlaid segmented 3-D preoperative images onto video images of the patient [16]. This approach presented largely the same calibration and tracking problems as DiGioias system, and in addition, the projected image also had to be warped to conform to the surface of the patient. Iseki et al. created a volumetric overlay display, and off-line registered to the patient in intracranial neurosurgery cases with the use of fiducials implanted into the skull [19, 29]. Current volumetric augmented reality devices require painstaking calibration and real-time spatial tracking with the limitations described above, and most current systems depend on complex and expensive hardware.

2 SYSTEM IMPLEMENTATION

2.1 Design

The system concept for the image overlay is shown in Fig. 1. A flat-panel display is aligned with a semi-transparent mirror; this unit is mounted in the mouth of an imaging scanner that is able to produce 2D transverse (axial) slices. Typically, the patient is translated out of the bore with the encoded table to position the body under the overlay unit. In short-bore or open scanners, the overlay may be able to coincide with the scan plane. The scanner, display, and mirror are co-aligned so that the reflection of a transverse image appearing in the mirror coincides with the patient's body behind the mirror. The image appears to be floating inside the patient, as if the operator had "tomographic vision" by virtually slicing the body. A virtual needle guide is chosen along the specified trajectory, and this guide is superimposed on the overlaid anatomical image. The clinician then inserts the needle using the overlaid guide while simultaneously being able to see the anatomy and the patient; therefore, focus never has to be taken off the patient during the procedure. Our prior work on development of the MR image overlay is described in [14].

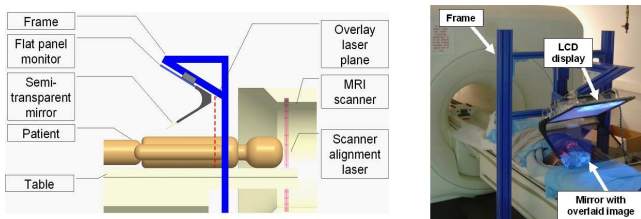


Figure 1: System concept of 2D image overlay device (left) and MR image overlay device in cadaver trial (right).

In earlier work, we investigated CT-guided needle insertion with 2D image overlay, which is similar to the current MR design. A detailed description of the application and analysis of the 2D image overlay technique as applied to CT guidance is described in [12, 13]. Also, Stetten et al. have shown a similar 2D overlay technique with applications to ultrasound [37].

Our image overlay system displays transverse MR images on an LCD display, which are reflected back to the physician from a semi-transparent mirror. For the CT-compatible version, oblique images can be used with no change in the workflow because the overlay tilts with the gantry as a single rigid body. For MR, the limitation to axial images comes from the lack of the required degrees of freedom to adjust the overlay in the current system; encoded rotations

will allow oblique images to be displayed in the upcoming revision. Looking through this mirror, the MR image appears to be floating in the correct location in the body. The intersection of the mirror and display surface planes is marked with a transverse laser plane that is used for constraining the needle to the image plane. The MR overlay system is realized by fixing an MR-compatible LCD screen that is housed in an acrylic shell to a semi-transparent mirror at a precise angle of 60° . (This angle can be changed, but the critical factor is to match the angle between the LCD and mirror to that between the mirror and the image plane.) The overlay unit is suspended from a modular extruded fiberglass frame as in Fig. 1 (right). The free-standing frame arches over the scanner table and allows for images to be displayed on a patient when the encoded couch is translated out of the bore by a known amount. To maintain the goal of a very practical and low cost system, an off-the-shelf 19" LCD display was retrofitted to be MRI safe and electromagnetically (EM) shielded. The "home made" MR display functions adequately up to 1m from the scanner bore on a 1.5T scanner; this allows for sufficient access to the patient by translating the encoded table out as described later in Section 2.3.

To use the system, a small stack of transverse images are acquired and one is selected as the guidance image. The software flips the image as required, adjusts its in-plane orientation and magnification, superimposes additional guidance information (e.g. virtual needle guide, ruler and labels), and renders the modified image on the flat panel display. Perhaps the most attractive feature of the image overlay system is that the operator has optical guidance in executing the intervention without turning his/her attention away from the field of action, while performing the same actions as in conventional freehand procedures. A close up view of the overlay system during a procedure is shown in Fig. 2. In most needle placement procedures, after the entry point is selected with the use of skin fiducials, the operator must control three degrees-of-freedom (DOF) needle motion. In this case, the operator uses the overlay image to control the in-plane insertion angle (1st DOF), while holding the needle in the transverse plane marked by a laser light (2nd DOF). The insertion depth (3rd DOF) may be marked with a clamp and/or zebra scale (circumferential marks) on the needle; the overlay display also provides a ruler and a depth gauge. The traditional unassisted procedure, to which operators are accustomed, is not altered; it rather increases the amount of visual information in the field of action. As the majority of needle placement procedures are executed "in-plane" (i.e. when the needle is completely contained in a single image slice), giving up full 3D rendering for engineering simplicity and low cost appears to be a most reasonable tradeoff. The overlay can also help detect target motion and allow for gating the needle insertion by the respiratory cycle. (The needle is advanced forward only when the fiducials on the patient and in the overlay image coincide at the peak of the respiratory cycle.) To account for needle bending, target motion, or to increase safety around critical structures, needles can be incrementally inserted with repeated imaging to verify the current trajectory and changes can be made as necessary.

In summary, the main advantages of the MR image overlay system as compared to traditional techniques are: (1) Planning image is available for intra-procedural guidance; (2) Physical patient, MR image, needle, and insertion plan are rendered in a single view, (3) Optically stable images are provided without auxiliary tracking instrumentation; (4) Only simple alignment is required; (5) System is inexpensive; (6) Same view is shared by multiple observers.

2.2 Calibration

Calibration is accomplished in three stages: 1) align the overlay image such that it coincides with the plane of the overlay system's laser plane, 2) align the overlay system such that its laser plane is parallel to the scanner's transverse imaging plane, and 3) determine

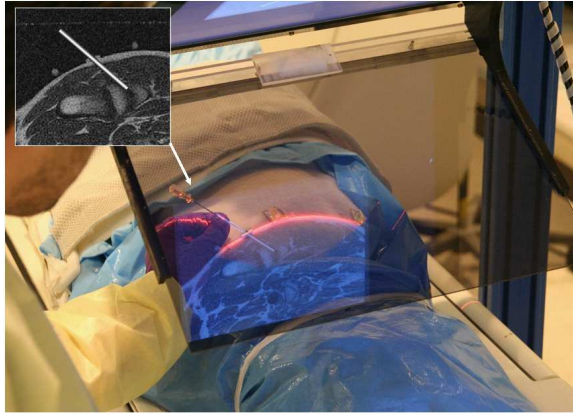


Figure 2: Close up view of the MR image overlay system in a porcine trials for guiding needle insertions into the joint space of the shoulder. The plan on the targeting image is shown in the inlay.

the in-plane transformation between the overlaid MR image and the view of the physical object in the mirror.

The initial stage of calibration is performed during manufacturing of the device to guarantee that the angle between the laser plane and the mirror and the mirror and the LCD are the same (60°). The laser is adjusted such that it passes through the intersection of the LCD and mirror planes while maintaining the correct angle with respect to the mirror (60°). This alignment is performed on a stable optical table with a digital level that provides an accuracy of better than 0.5° . The second stage is performed when the overlay system is brought into the scanner room. To ensure parallelism of the scanner's image plane and overlaid image, a calibration phantom is manually adjusted on the MR table until the scanner's transverse laser plane sweeps the front face of the fiducial board; the scanner bed is then translated out and the overlay is positioned such that its onboard laser line generator does the same.

The first step of the in-plane registration stage is image scaling. The overlay image must appear in correct size in the mirror, but there is variable linear scaling between the MR image and displayed image. The pixel size of the display is constant and it is either known from the manufacturer's specification or its measurement is trivial. The pixel size of the MR image is extracted from the DICOM header or calculated as the ratio between the field of view (in millimeters) and image size (in pixels). The second step of in-plane registration is to determine a 3-DOF rigid body transformation. An MR image of either a calibration phantom or of the patient him or herself with fiducials placed on the skin is acquired, and the image is rendered on the overlay display as seen in Fig. 3. The in-plane rotation and translation of the overlaid image is adjusted until each fiducial marker coincides with its mark in the image. This calibration process is similar to that of the CT Image Overlay which is described in depth in [12, 13].

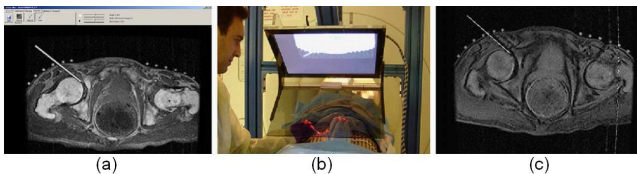


Figure 3: MR image overlay guided direct MR arthrography in cadaver trials. Targeting image with overlaid guide (a) insertion under overlay guidance (b) and confirmation image with overlaid targeting plan (c).

2.3 Workflow

In order to increase patient safety and reliability in data reporting, the calibration and system setup may be verified before each experiment and especially before treating each individual patient. Assuming a pre-procedurally aligned system, the intra-procedure workflow is as follows:

- Place the patient on the table and place imaging coil over the target site.
- Prepare the site of intervention and place sterile skin fiducial (TargoGrid from Invivo Corp., Orlando, FL) with the parallel bars orthogonal to the approximate slice direction.
- Translate the patient into the scanner and acquire a thin slab of MRI images with appropriate slice thickness for lesion conspicuity.
- Transfer the image directly in DICOM format to the planning and control software implemented on a stand-alone PC; select the target of interest and the percutaneous puncture point as shown in Fig. 3(a).
- Display a visual guide along the trajectory of insertion and render the image on the overlay device.
- Translate out the table with the patient such that the selected entry point is under gantry's laser plane and mark the plane and/or entry point; continue to translate out the table such that the marked entry point is under overlay's laser plane.
- Verify the alignment of the overlay image to the patient, and update the in-plane alignment as described in Section 2.2 if any changes in configuration were made since the previous insertion.
- Take the needle in hand, reach behind the mirror, touch down on the selected entry point, and rotate the needle to match with the virtual guide while keeping it in the laser plane as shown in Fig. 3(b).
- Verify that the respective fiducials on the patient and in image coincide; the skin fiducials can be used to gate or synchronize the needle insertion to the respiratory cycle.
- Insert the needle to the predefined depth while maintaining in plane and out of plane alignment.
- Translate the patient back into the scanner and acquire a confirmation image (Fig. 3(c)); if the needle position is satisfactory, perform the rest of the intervention (contrast injection, harvest tissue sample, etc.)

3 EXPERIMENTS AND RESULTS

3.1 Cadaver Trials

The MR overlay system as shown in Fig. 1 (right) has been successfully tested in 1.5T and 3T scanners for compatibility. Joint arthrography needle insertions have been performed under MR image overlay guidance on porcine and human cadavers in a 1.5T GE Signa scanner using the workflow described in Section 2.3. In the porcine cadaver trials, twelve separate insertions were performed in the joint space of the shoulder of three fresh (within one hour of euthanasia in unrelated studies) porcine cadavers. Insertions were performed using 18G, 10cm MR-compatible needles (EZ-EM Inc., Lake Success, NY) with insertion depths ranging from 26-43mm. In the human cadaver trials, ten separate insertions were performed in the joint space of the hip of two cadavers. Again, insertions

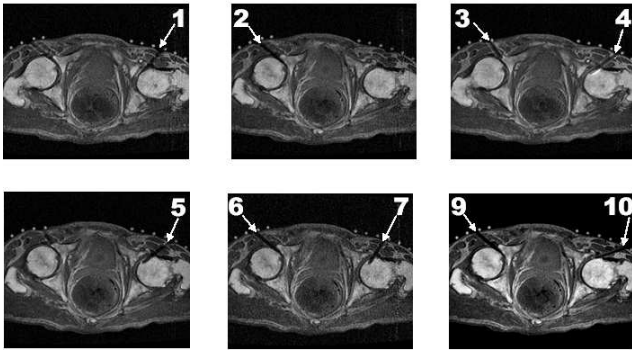


Figure 4: Results from ten needle insertions into the joint space of the hip on human cadavers under MR image overlay guidance.

were performed using 18G, 10cm MR-compatible needles; insertion depths ranged from 30-54mm. Planning and confirmation images from both sets of trials were examined by two board certified radiologists to determine whether the tip of the needle landed in the joint space. The needles were successfully inserted into the joint on the first attempt in all cases. An example is shown in Fig. 4; determining the exact placement of the needle is difficult in these images due to paramagnetic artifact from the needle and the 4mm slice thickness. Quantitative accuracy analysis was not possible due to the relatively large artifact in the MR images and the lack of distinct target points.

To demonstrate the ability for guiding percutaneous spinal access, needle insertions have been performed with the MR image overlay on an interventional abdominal phantom (CIRS Inc., Norfolk, VA). Successful access of all anatomical targets was verified in MRI visually; needle artifact and lack of distinct targets again did not allow for precise error measurement. To further verify image overlay capabilities, successful insertions with depths of up to 100mm have been performed in porcine cadavers. Functionally similar earlier trials with a CT image overlay (where exact target verification and accuracy assessment is possible) have proven the technique reliable for guiding percutaneous access on human and porcine cadavers [12, 13].

3.2 Comparison of Four Techniques

To further validate the efficacy and accuracy of MR image overlay guidance, four manual needle insertion techniques were compared:

1. Image overlay as described above and in [14] (Fig. 5(a))
2. Biplane laser that marks the insertion bath with the intersection of two calibrated laser planes as described in [15] (Fig. 5(b))
3. Handheld protractor with pre-angled guide sleeve (Fig. 5(c))
4. Conventional freehand needle insertion

All techniques feature translating patient out of the scanner for insertion, skin fiducials to determine puncture point, and manual needle placement in laser-marked transverse plane. All four are equivalent in controlling out-of-plane angle and depth; therefore, these aspects were not evaluated.

Three series of experiments were conducted with 1.5T GE Signa scanner and 18G MR-compatible beveled needles. The first trial used a CIRS abdominal phantom with TargoGrid fiducials as shown in Fig. 5 (a-c); four needle insertions were performed for each technique. In this test, the procedure was performed on the MRI scanner and MRI-based validation was used. All insertions were

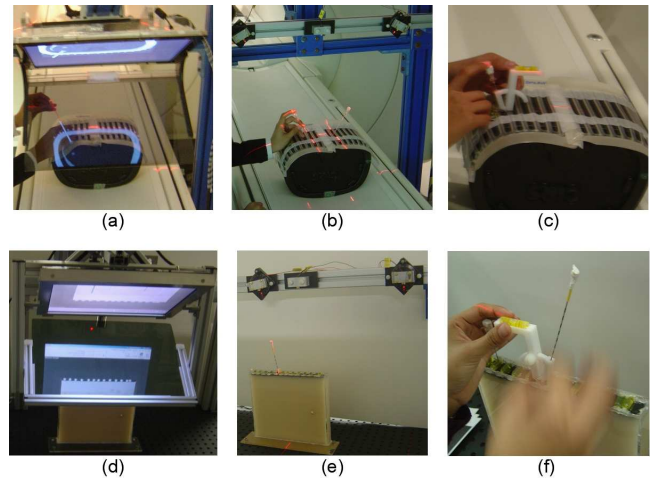


Figure 5: Comparison studies between MR image overlay (a,d), biplane laser guide (b,e), handheld protractor guide (c,f), and traditional freehand. Initial studies were performed under MR imaging (a-c) and follow up quantitative comparisons were performed the laboratory with a functionally equivalent system configuration (d-f).

visually successful, but needle artifact and lack of distinct targets rendered quantitative measurement inconclusive. A follow-up trial was performed similarly, but four separate needle insertion phantoms were used (one for each technique); these phantoms are of the same type as the last experiment. In this experiment, the same three needle insertions were performed with each technique in the MR scanner, and accuracy measurements were made independently using fluoroscopy as shown in Fig. 6. Although the results are not statistically significant due to the small sample size, the average error between the needle and the target was less than 2mm for the image overlay; the other techniques ranged in accuracy from 2.6mm to 7.4mm (for freehand). These first two experiments serve as a proof-of-concept for all four techniques in the MR environment.

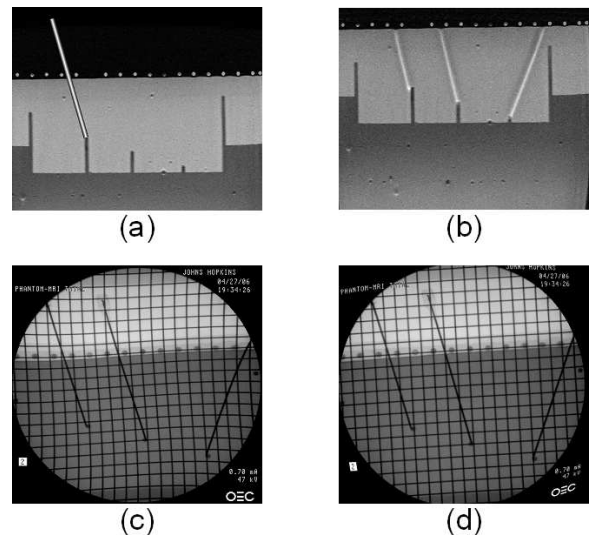


Figure 6: Needle insertion validation procedure for MR image overlay phantom trials using fluoroscopy. A plan is generated and displayed on the overlay (a), the needle is inserted and a confirmation MR image is acquired (b), the phantom is placed in a c-arm fluoroscope and a fluoroscopic image is acquired (c), and measurements are made on a dewarped version of the fluoroscopic image (d).

The third experiment used a phantom filled with two different stiffness layers of tissue-equivalent gel and five embedded 4mm plastic targets, and covered with neoprene skin. This test was performed based on MR images, but conducted on a functionally equivalent configuration of the devices in a laboratory setting as shown in Fig. 5(d-f). A total of 30 insertions were performed with each technique; C-arm fluoroscopy was used to determine in-plane tip position error and angular error. This experiment serves as a quantitative comparison in the laboratory of the four techniques. Results from this trial are shown in Figure 7. Technique made a significant difference in tip position error ($p=0.015$) and angle error ($p=0.053$). With a 75% confidence interval, biplane laser and image overlay provide for better tip placement accuracy than the other techniques. With an 80% confidence interval, biplane laser and image overlay have better angular accuracy than the other techniques. In terms of angular and positional accuracies, no significant difference was found between the laser guide and image overlay in these preliminary studies.

Technique	Avg. Pos. Error (mm)	Std. Dev. Pos. Err.	Avg. Ori. Err. (deg)	Std. Dev. Ori. Err.
Freehand	5.27	5.56	4.07	4.11
Protractor	5.37	7.36	3.35	3.34
Laser	2.90	2.62	2.02	2.22
Overlay	2.00	1.70	2.41	2.27

Figure 7: Results from quantitative comparison between the three assisted techniques and traditional freehand in the equivalent laboratory system configuration. In-plane needle insertion accuracy is presented for four techniques with 30 insertions each.

4 DISCUSSION

Initial cadaver and phantom experiments support the hypothesis that the MR image overlay can provide accurate needle placement while significantly simplifying the arthrography procedure by eliminating separate radiographically guided contrast injection. The system also appears to be useful in spinal needle placement, however, independent measurement of accuracy will have to support this claim in later trials. In our studies, by visualizing target anatomy and providing a visual guide, the MR image overlay allowed for accurate needle placement on the first attempt consistently.

There were many lessons learned and hurdles overcome in the development of this system. The first hurdle was transitioning the CT-compatible system to MRI, which required ensuring MR compatibility of the flat panel display. The current display is standard LCD display that had the steel casing removed and replaced with aluminum EM shielding. The current display can function adequately up to 1m from the scanner bore before saturation of the ferrite core inductors; we are investigating options that will allow the overlay unit to be moved in closer proximity to the scanner. Another issue that arises with 2D image overlay in general is parallax as described in [12]; the key is to optimize the parallax error by decreasing the thickness of the mirror, while maintaining rigidity of the mirror to eliminate sagging. We have settled on 4mm thick smoked acrylic sheets as the semi-transparent mirror material. Visibility of the overlaid image on the mirror is dependent on the room lighting; we have found that dimming the lights enhances the overlaid image, but in turn decreases the visibility of the patient and the needle behind the mirror. Typically the lights behind the clinician are dimmed while maintaining illumination on the opposite side; the optimal configuration appears to be based on user preference. Calibration of the device is an aspect that has evolved significantly from our early attempts at 2D image overlay. We used to believe that a full calibration of the in plane alignment was necessary during initial set up of the system on the scanner. The current

procedure involves simply aligning the image in the overlay with the skin fiducials on the patient; this is faster by eliminating a step, simpler to perform, and safer since it guarantees alignment of the guide with the patient at the time of insertion. Further, this eliminates the need for a special calibration phantom for alignment with the patient as described in Section 2.2; we can use any object with a flat vertical face to ensure parallelism between the system and the scanner during system setup.

During the experiments, it was revealed that holding the needle in the plane of insertion can be difficult, especially for non-expert users. We attempted to ease this problem with a mechanical needle guide; a horizontal bar was attached to the display-mirror unit, shown in Fig. 8(a). The bar is made of acrylic and its height is adjustable. The operator places the needle at the skin entry point and presses the needle gently against the bar while inserting the needle. Although not yet implemented, a stronger constraint can be provided by adding a sliding-rotating needle guide with a quick release mechanism shown in Fig. 8(b). Although mechanical constraints are redundant in addition to optical guidance, they appear to be very useful for increasing the level of comfort and confidence of some operators. Preliminary results suggested that as the user becomes more accustomed to the image overlay device, the benefits of mechanical constraints are reduced and can in fact become a hindrance. IRB approval has just recently been granted to perform large scale trials with phantoms to determine the optimal combination of visual and mechanical assistance. We will conduct extensive operator motion and performance analysis, as well as human machine interface ergonomics studies. IRB approval was needed because the "human subjects" in these studies will be the operators. In upcoming phantom trials in the laboratory, we plan to use electromagnetically tracked needles for measuring placement accuracy as opposed to fluoroscopic imaging; this will allow for more consistent results and also the ability to measure placement error precisely with respect to anatomical targets.

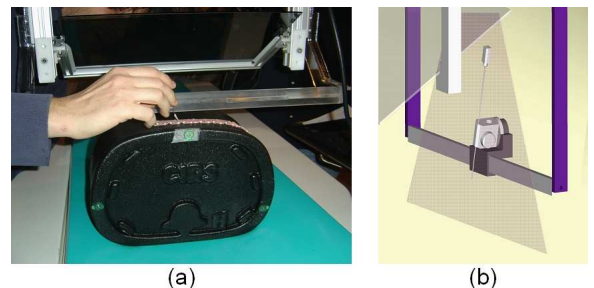


Figure 8: Mechanical needle guide for maintaining the needle orientation in the image plane (shown with the CIRS abdominal phantom) (a), and design of an adjustable angle needle guide to maintain both in plane and out of plane orientation (b).

From the comparison studies, enhanced needle insertion techniques appear to provide substantial benefit over conventional needle insertion. In the relatively straightforward phantom experiment, biplane laser and image overlay guidance performed similarly. For cases where it is unnecessary to see the target anatomy, the biplane laser appears adequate. However, when visualization of the target anatomy is preferred, such as when performing needle placement in the joints or other musculoskeletal targets, the image overlay provides significant benefits over other techniques.

Presently, IRB approval is being sought to commence clinical trials for MR image overlay guided joint arthrography. The current overlay system is limited to the transverse plane. Concurrently, a dynamic overlay system is in development, which will be smaller in size and moved over the body to allow for needle insertion in arbitrary tilted planes, thereby significantly increasing the flexibility and user friendliness of the system.

The authors would like to acknowledge Iulian Iordachita for assistance in manufacturing, Daniel Schlattman for help with shielding the LCD display and Hugh Wall for help with the scanner. Partial funding for this project was provided by NSF Engineering Research Center Grant #EEC-97-31478, Siemens Corporate Research and William R. Kenan, Jr. Fund.

REFERENCES

- [1] Bergin D, Schweitzer ME. Indirect magnetic resonance arthrography. *Skeletal Radiol*, Oct 2003; 32(10):551–8.
- [2] Binkert CA, Verdun FR, Zanetti M, Pfirrmann CW, Hodler J. CT arthrography of the glenohumeral joint: CT fluoroscopy versus conventional CT and fluoroscopy—comparison of image-guidance techniques. *Radiology*, 2003; 229(1):153–158.
- [3] Birkfellner H, Figl W, Huber M, et al. A head-mounted operating binocular for augmented reality visualization in medicinedesign and initial evaluation. *IEEE Trans Med Imag*, Aug 2002; 21(8):991–997.
- [4] Blackwell M, Nikou C, DiGioia AM, Kanade T. An image overlay system for medical data visualization. *Proc 1st Int Conf Med Image Computing and Computer-Assisted Intervention*, 1998; LNCS 1496:232–240.
- [5] Bock M, et al. Combination of a Fully MR-compatible Robotical Assistance System for Closed-bore High-field MRI Scanners with Active Device Tracking and Automated Image Slice Positioning. *RSNA*, 2004.
- [6] Chinzei K, Miller K. Towards MRI guided surgical manipulator. *Med Sci Monit*. 2001 Jan-Feb; 7(1):153–63.
- [7] Cleary K, Nguyen C. State of the art in surgical robotics: clinical applications and technology challenges. *Computer Aided Surgery*, 2001; 6(6):312–328.
- [8] DiGioia AM, Colgan BD, Koerber N. Computer aided surgery. *Cyber-surgery*, 1998; 121–139.
- [9] DiMaio S, Fischer G, Haker S, Hata N, Iordachita I, Tempany C, Fichtinger G. Design of an Prostate Needle Placement Robot in MRI Scanner. *IEEE Int Conf on Biomedical Robotics*, Feb 2006.
- [10] Edwards PJ, et al. Design and Evaluation of a System for Microscope-Assisted Guided Interventions (MAGI). *IEEE Trans. Med. Ing.*, Nov 2000; 19(11):1082–1093.
- [11] Fahrig R, Butts K, Rowlands JA, et al. A truly hybrid interventional MR/X-ray system: feasibility demonstration. *J Magn Reson Imaging*, Feb 2001; 13(2):294–300.
- [12] Fichtinger G, Deguet A, Masamune K, Fischer GS, Balogh E, Mathieu H, Taylor RH, SJ Zinreich, Fayad LM. Image Overlay Guidance for Needle Insertions in CT Scanner. *IEEE Transactions on Biomedical Engineering*, 2005; 52:1415–1424.
- [13] Fichtinger G, Deguet A, Fischer GS, Balogh E, Masamune K, Taylor RH, Fayad LM, SJ Zinreich. CT Image Overlay for Percutaneous Needle Insertions. *Journal of Computer Aided Surgery*, July 2005; 10(4):241–255.
- [14] Fischer GS, Deguet A, Schlattman D, Taylor RH, Fayad L, Zinreich SJ, Fichtinger G. MRI image overlay: applications to arthrography needle insertion. *Studies in health technology and informatics - Medicine Meets Virtual Reality 14*, 2006; 119:150–155.
- [15] Fischer GS, Wamsley C, Zinreich SJ, Fichtinger G. Laser-Assisted MRI-Guided Needle Insertion and Comparison of Techniques. *Int Soc for Comp Asst Orthopaedic Surg*, Jun 2006.
- [16] Grimson WEL, Ettinger GJ, White SJ, Lozano-Perez L, Wells III WM, Kikinis R. An automatic registration method for frameless stereotaxy, image guided surgery, and enhanced reality visualization. *IEEE Trans Med Imag*, Apr 1996; 15(2):129–139.
- [17] Hata N, et al. Needle guiding robot for MR-guided microwave thermotherapy of liver tumor using motorized remote-center-of-motion constraint. *5th Interventional MRI Symposium*. Oct 2004.
- [18] Hilfiker PR, Weishaupt D, Schmid M, Dubno B, Hodler J, Debatin JF. Real-time MR-guided joint puncture and arthrography. *Eur Radiol*, 1999; 9(2):201–204.
- [19] Iseki H, Masutani Y, Iwahara M, et al. Volumegraph (overlaid three-dimensional image-guided navigation), Clinical application of augmented reality in neurosurgery. *Stereotact Funct Neurosurg*, 1997; 68:18–24.
- [20] Jolesz FA. Interventional and intraoperative MRI: A general overview of the field. *J Magn Reson Imaging*, 1998; 8(1):3–7.
- [21] Jolesz FA, Talos IF, Schwartz RB, et al. Intraoperative magnetic resonance imaging and magnetic resonance imaging-guided therapy for brain tumors. *Neuroimaging Clin N Am*, 2002 Nov; 12(4):665–683.
- [22] Kockro RA, Serra L, Tseng-Tsai Y, et al. Planning and simulation of neurosurgery in a virtual reality environment. *Neurosurgery*, 2000; 46(1):118–135.
- [23] Kreitner KF, Loew R, Runkel M, Zollner J, Thelen M. Low-field MR arthrography of the shoulder joint: technique, indications, and clinical results. *Eur Radiol*, Feb 2003; 13(2):320–329.
- [24] Krieger A, Susil RC, Menard C, Coleman JA, Fichtinger G, Atalar E, Whitcomb LL. Design of A Novel MRI Compatible Manipulator for Image Guided Prostate Intervention. *IEEE Trans Biomed Eng*, 2005; 52(2):306–313.
- [25] Lenchik L, Dovgan DJ, Kier R. CT of the iliopsoas compartment: value in differentiating tumor, abscess, and hematoma. *Am J Roentgenol*, 1994; 162:83–86.
- [26] Lewin JS, Petersilge CA, Hatem SF, et al. Interactive MR imaging-guided biopsy and aspiration with a modified clinical C-arm system. *Am J Roentgenol*, 1998; 170:1593–1601.
- [27] Lewin JS, Nour SG, Duerk JL. Magnetic resonance image-guided biopsy and aspiration. *Top Magn Reson Imaging*, 2000; 11(3):173–183.
- [28] Masamune K, Inagaki T, Takai N, Suzuki M. Needle Insertion Manipulator MRI Compatible Needle Insertion Manipulator and Image Distortion Measurement for the Evaluation. *J JSCAS*, 2001; 3(4):273–280.
- [29] Nakajima S, Nakamura K, Masamune K, Sakuma I, Dohi T. Three-dimensional medical imaging display with computer-generated integral photography. *Computer. Med. Imag. Graph.*, 2001; 25:235–241.
- [30] Ojala R, Klemola R, Karppinen J, Sequeiros RB, Tervonen O. Sacroiliac joint arthrography in low back pain: feasibility of MRI guidance. *Eur J Radiol*, 2001; 40(3):236–239.
- [31] Petersilge CA, Lewin JS, Duerk JL, Hatem SF. MR arthrography of the shoulder: rethinking traditional imaging procedures to meet the technical requirements of MR imaging guidance. *AJR Am J Roentgenol*, Nov 1997; 169(5):1453–1457.
- [32] Salomonowitz E. MR imaging-guided biopsy and therapeutic intervention in a closed-configuration magnet: single-center series of 361 punctures. *Am J Roentgenol*, 2001; 177(1):159–163.
- [33] Sauer F, Khamene A, Vogt S. An augmented reality navigation system with a single-camera tracker: system design and needle biopsy phantom trial. *Proc 5th Int Conf Med Image Computing and Computer-Assisted Intervention*, 2002; LNCS 2489:116–124.
- [34] Schmitt R, Christopoulos G, Meier R, Coblenz G, Frohner S, Lanz U, Krimmer H. Direct MR arthrography of the wrist in comparison with arthroscopy: a prospective study on 125 patients. *Rofo*, Jul 2003; 175(7):911–9.
- [35] Schulte-Altendorfer G, Gebhard M, Wohlgemuth WA, et al. MR arthrography: pharmacology, efficacy and safety in clinical trials. *Skeletal Radiology*, 2003; 32:1–12.
- [36] Steinbach LS, Palmer WE, Schweitzer ME. Special focus session, MR arthrography. *Radiographics*, Sep-Oct 2002; 22(5):1223–1246.
- [37] Stetten GD, Chib VS. Overlaying ultrasonographic images on direct vision. *J Ultrasound Med*, 2001; 20(3):235–240.
- [38] Taylor RH, Stoianovici D. Medical robotics in computer-integrated surgery. *IEEE Trans Robot Automat*, May 2003; 19(5):765–781.
- [39] Trattng S, Breitenseher M, Pretterkieber M, Kontaxis G, Rand T, Helbich T, Imhof H. MR-guided joint puncture and real-time MR-assisted contrast media application. *Acta Radiol*, Nov 1997 Nov; 38(6):1047–1049.
- [40] Trattng S, Breitenseher M, Rand T, Bassalamah A, Schick S, Imhof H, Petersilge CA. MR imaging-guided MR arthrography of the shoulder: clinical experience on a conventional closed high-field system. *AJR Am J Roentgenol*, Jun 1999; 172(6):1572–1574.
- [41] Zoga AC, Schweitzer ME. Indirect magnetic resonance arthrography: applications in sports imaging. *Top Mag Res Img*, 2003; 14(1):25–33.